ChemPubSoc Europe

DOI: 10.1002/cssc.201600961

CHEMSUSCHEM Full Papers

Direct Hydrogen Evolution from Saline Water Reduction at Neutral pH using Organic Photocathodes

Marta Haro[+],[a] Claudia Solis[+],[b] Vicente M. Blas-Ferrando,[a] Olivier Margeat,[c] Sadok Ben Dhkil,[c] Christine Videlot-Ackermann,[c] Jörg Ackermann,[c] Fabio Di Fonzo,[d] Antonio Guerrero,*[a] and Sixto Gimenez*[a]

Here, we have developed an organic photocathode for water reduction to H_2, delivering more than 1 mA cm^{-2} at 0 V versus RHE and above 3 mA cm^{-2} at −0.5 V versus RHE with moderate stability under neutral pH conditions. The initial competitive reduction of water to H_2 and ZnO to metallic Zn is responsible for the dynamic behaviour of both photocurrent and Faradaic efficiency of the device, which reaches 100% Faradaic efficiency after 90 min operation. In any case, outstanding stable H_2 flow of approximately 2 μmol h^{-1} is measured over 1 h at 0 V versus RHE and at neutral pH, after equilibrium between the Zn^{2+}/Zn^0 concentration in the AZO film is reached. This achievement opens new avenues for the development of all-solution-processed organic photoelectrochemical cells for the solar generation of H_2 from sea water.

Introduction

The present energy context urgently demands the availability of sustainable and renewable resources to meet the needs of a growing world population with increasing living standards and hence high energy demand.[1] Chemical fuels constitute an attractive energy vector, as they can be easily stored and used upon demand.[2] Consequently, large-scale generation of chemical fuels from decentralized and sustainable resources, like water and sun, is considered one of the key challenges for science and technology. In this context, photoelectrochemical generation of solar fuels with semiconductor materials is a promising approach towards the direct conversion of solar energy into chemical fuels.[3] Indeed, competitive solar-to-hydrogen efficiencies over 10% have been reported for different device architectures using this approach.[4] However, recent techno-economic analysis predicted that the future implementation of this technology will depend on the feasibility of efficient and durable devices targeting $2–4 kg^{-1} of dispensed H_2.[5] This stringent cost-requirement places low-cost materials and synthetic strategies at the forefront of the research in the field. Additionally, commercial systems should be capable of producing H_2 from seawater without any chemical bias.

Semiconducting organic materials (particularly conjugated polymers) have been thoroughly exploited in the field of optoelectronics and photovoltaics. These materials can be processed from solution techniques compatible with low cost manufacturing, such as roll-to-roll processing.[6] Indeed, solar-to-electricity efficiencies around 10% have been achieved for organic photovoltaic (OPV) devices.[7] In contrast, these materials have not received comparable interest for the generation of solar fuels for decades. The first report demonstrating that conjugated polymers can photocatalyze H_2 evolution in aqueous solutions containing sacrificial systems was carried out by Yanagida in 1985.[8] Since then, only a few studies have explored the use of these materials for photoelectrochemical generation of solar fuels.[9] In general, immersing organic photoelectrodes in liquid solutions systematically led to very low photocurrents (≈1 μA cm^{-2}) under application of light and electrical bias and the poor stability of these devices rendered reasonable doubts on the origin of the photocurrent. However, it was recently showed that interfacing an OPV with a liquid solution (0.1 M tetrabutylammonium hexafluorophosphate solution in acetonitrile with a redox pair able to capture either electrons or holes) does not deleteriously affect the photocurrent that the device can deliver in a solid-state configuration, and quantitative photocarrier conversion has been demonstrated.[10]

[a] Dr. M. Haro,[+] Dr. V. M. Blas-Ferrando, Dr. A. Guerrero, Dr. S. Gimenez
Institute of Advanced Materials (INAM)
Universitat Jaume I
12071 Castelló (Spain)
E-mail: aguerrer@uji.es
sjulia@uji.es

[b] Dr. C. Solis[+]
Universidad Nacional Rio Cuarto
Departamento de Química
X5804BYA, Río Cuarto (Argentina)

[c] Dr. O. Margeat, Dr. S. B. Dhkil, Prof. C. Videlot-Ackermann, Prof. J. Ackermann
Aix-Marseille Université
CNRS, CINaM UMR 7325
13288 Marseille (France)

[d] Dr. F. Di Fonzo
Center for Nano Science and Technology@PoliMi
Istituto Italiano di Tecnologia
Via Pascoli 70/3
20133 Milano (Italy)

[+] Both authors have equally contributed to this work.

Supporting Information and the ORCID identification number(s) for the author(s) of this article can be found under http://dx.doi.org/10.1002/cssc.201600961.

Focusing on organic photocathodes for water reduction, some inspiring studies have highlighted the potential of OPVs in acidic environments (pH ~ 1) and a rapid increase of photocurrent from hundreds of $\mu A\,cm^{-2}$ to some $mA\,cm^{-2}$ has been obtained.[11] The basic strategy behind this impressive progress entails the optimization of hole and electron selective contacts to deliver maximum photocurrents, while providing reasonable stability for long-term application. Interestingly, organic photoanodes for water oxidation based on conjugated polymers have been recently reported,[12] opening promising perspectives for the development of all-organic tandem photoelectrochemical water splitting cells.

In a previous study,[11d] we reported stable water reduction photocurrents of $\approx 250\,\mu A\,cm^{-2}$ for more than 3 h (pH 2) by using a cross-linkable poly(3,4-ethylenedioxythiophene)-poly(styrenesulfonate) (x-PEDOT:PSS) as the hole-selective layer and a TiO_x/Pt catalytic electron-selective layer sandwiching an archetypical bulk heterojunction (BHJ) blend of poly(3-hexylthiophene) (P3HT) and phenyl-C61-butyric acid methyl ester (PCBM). The high resistance of the synthesized TiO_x layer has motivated the exploration of more conductive electron-selective layers compatible with operation at neutral pH. In the present study we developed an Al-doped ZnO (AZO) electron-selective layer prepared by a novel process compatible with low temperature synthesis. We show photocurrents above $1\,mA\,cm^{-2}$ at 0 V versus RHE (V_{RHE}) and above $3\,mA\,cm^{-2}$ at $-0.5\,V_{RHE}$ with moderate stability at neutral pH conditions, when a C/Pt catalyst is deposited on top of the device. The Faradaic efficiency of the device for water reduction to hydrogen increases with time from 60% up to 100% owing to the competitive partial reduction of the selective ZnO layer to metallic Zn. Although other studies have reported interesting efficiencies for water reduction at neutral pH, they rely on more sophisticated photovoltaic technologies (e.g., CIGS), which employ high-temperature and high-vacuum processing.[13] Consequently, the achievements of the current work open new avenues for the development of all-solution-processed photoelectrochemical cells for the solar generation of H_2 from sea water.

The AZO nanocrystals were chemically synthesized through a solution approach that does not require bulky insulating ligands as surfactants, allowing the formation of thin films at a low 85 °C annealing temperature with improved conductivity compared to ZnO.[14] Figure 1a shows a TEM image of the AZO nanoparticles and Figure 1b shows an AZO film observed by SEM. The average diameter of these nanoparticles is 10 nm and they appear dispersed without agglomeration by dynamic light scattering measurements. The Al-doping level of 0.8% was determined by inductively coupled plasma mass spectrometry (ICP-MS) analyses. Powder X-ray diffraction (PXRD) patterns shown in the Supporting Information (Figure SI1) highlight the crystalline nature of the nanocrystals generated using this synthetic procedure. The work function is 4.08 eV with conduction band energy of 3.79 eV and ionization potential of 7.87 eV as determined in Ref. [14]. These values suggest that AZO is a promising candidate to be used as an electron-selective layer in organic photoelectrochemical devices and an

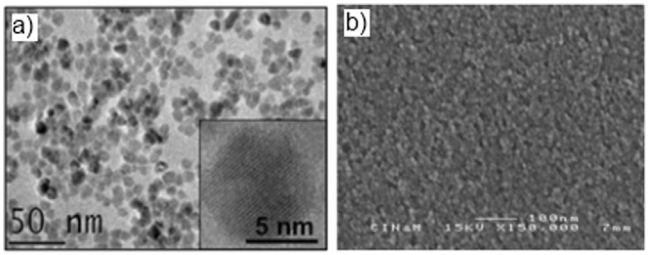

Figure 1. a) TEM and b) SEM images of the AZO nanoparticles.

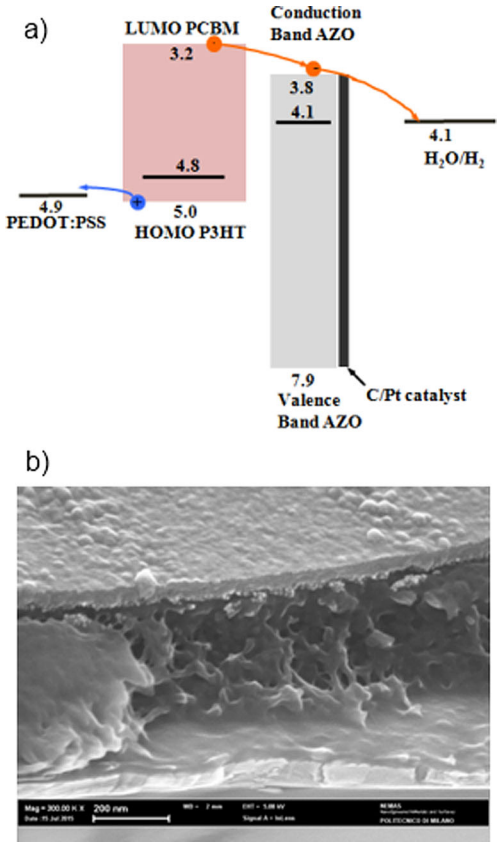

Figure 2. a) Energy diagram of the device with architecture ITO/*x*-PEDOT/BHJ/AZO/C/Pt and pathway for electrons resulting in water reduction to H_2. b) SEM of the cross-section of a full device.

illustrative energy diagram of the full device is showed as Figure 2a. Average mobility values of $\mu = 2\times10^{-5}\,cm^2Vs^{-1}$ were extracted from field-effect transistors measurements (see Figures SI2 and SI3 for details). Although this is not an extremely high value, it is adequate to be used in devices with a few tens of nanometers.

A representative cross-sectional micrograph of the full *x*-PEDOT/BHJ/AZO/C/Pt device is shown in Figure 2b. The AZO layer appears as a nanoparticulated film on top of the device, coated by a ~1 nm thick layer of the C/Pt catalyst. The thicknesses of the *x*-PEDOT, BHJ, and AZO layers have been estimated as 40, 300, and 40 nm, respectively. The C/Pt catalytic layer is below 1 nm and cannot be identified by SEM.

The full devices were tested for H_2 evolution under acidic conditions (pH 2 and 5) showing poor performance (after the

first cyclic voltammetry scan) and low stability as shown in Figure SI4. This is in good correlation with the Pourbaix diagram of ZnO.[15] Then, the photoelectrochemical behavior of the devices for water reduction at neutral pH (pH 7) was investigated. Figure 3a shows the current–voltage (*j–V*) curve under chopped illumination, achieving remarkable photocurrents of 1.2 mA cm^{-2} at 0 V_{RHE} and above 3 mA cm^{-2} at −0.5 V_{RHE}. At the most positive values of potential showed in Figure 3a, cathodic spikes indicative of electron accumulation are observed,[16] but at potentials more negative than 0 V_{RHE}, the spikes are not any longer visible, reflecting the fully faradaic nature of the photocurrent. Compared to the pure Pt catalyst, the use of C/Pt notably improves the performance of the photocathode (see Figure SI5). This enhanced behavior can be ascribed to two different reasons. First, the size of the Pt nanoparticles is reduced, as nanoparticle aggregation is hampered by the presence of the carbon layer.[17] On the other hand, the carbon layer acts as an efficient electron scavenger from the oxide film,[18] improving both the charge-transfer kinetics (catalytic efficiency) and the long-term stability. The stability of the devices was studied by chronoamperometric measurements at 0 V_{RHE} and the obtained results are shown in Figure 3b. After 60 min chopped illumination, the photocurrent decreases 50%, but from this time on, the decrease is much more moderate, around 5% over the next 60 min, as can be seen in Figure SI6.

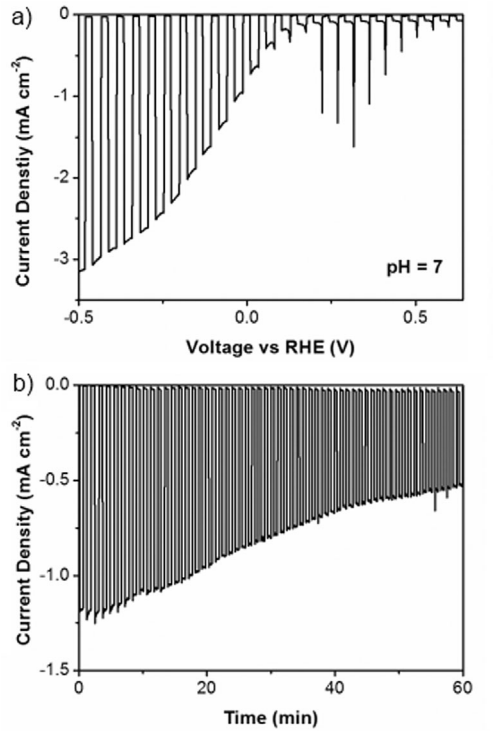

Figure 3. a) *j–V* plot for *x*-PEDOT/BHJ/AZO/C/Pt at pH 7 at a scan speed of 5 mV s^{-1}. b) *j–t* plot at V_{bias} = 0 V_{RHE}.

To gain insights into the time evolution of the photocurrent, surface characterization on pristine and aged devices (after 1 h testing at pH 7) was carried out by X-ray photoelectron spectroscopy (XPS, Figures 4 and SI7). Typical XPS spectra for the Zn 2p electrons before and after chronoamperometric testing are shown as Figure 4a and b, respectively. These spectra suggest some changes in the electronic structure of Zn. More conclusive information can be obtained from the Auger spectra showed in Figure 4c and d. The Zn $L_3M_{45}M_{45}$ Auger line measured with Al-Kα photons allows monitoring different Zn oxidation states, owing to the pronounced difference between positions and line shapes for both Zn and ZnO spectral components.[19] The results show that Zn is present as ZnO in the pristine sample, but a component of metallic Zn is detected after the chronoamperometric test, clearly indicating partial reduction of the metallic oxide upon operation under cathodic photocurrent. On the other hand, both the XPS spectra for

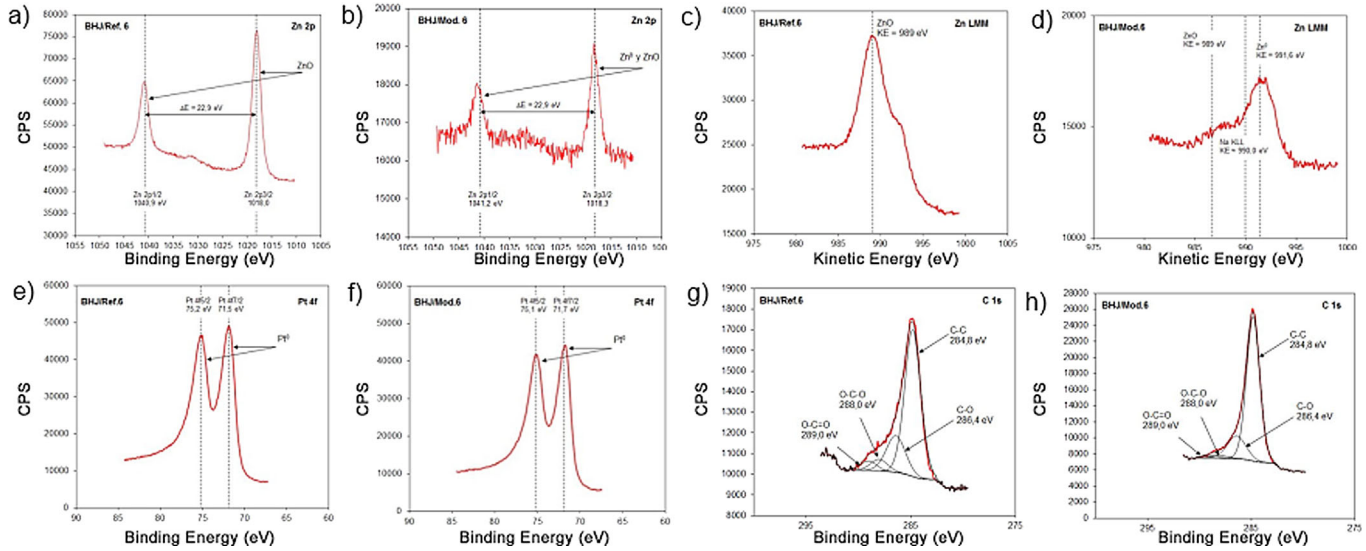

Figure 4. XPS spectra obtained from a *x*-PEDOT/BHJ/AZO/C/Pt device a, c, e) before and b, d, f) after chronoamperometric testing over 1 h at pH 7 under chopped illumination. a–b) Zn 2p signal, c–d) Zn Auger signal, e–f) Pt 4f signal, g–h) C 1s signal.

Pt 4f (Figure 4e–f) and C 1s (Figure 4g–h) show that the C/Pt catalyst does not suffer significant degradation during operation for 1 h at neutral pH.

Finally, H_2 production was evaluated by carrying out the measurements in a sealed cell where the output gas flow was periodically analyzed by gas chromatography, Figure 5a. Consistent with the results obtained from XPS (Figure 4), the electrode evolves during the first 90 min. Initially, the production of H_2 ($\approx$5 μmol h^{-1} cm^{-2}) is high, in agreement to the measured values of photocurrent. However, less than 60% of the photogenerated electrons are reducing water efficiently according to the calculated Faradaic efficiency. The rest of photogenerated electrons in the organic blend are injected into the AZO film with the subsequent Zn^{2+} reduction to Zn^0, as clearly suggested by Auger spectroscopy (Figures 4c–d). This behavior is more noticeable during the first 15 min. After this period, the photocurrent decreases while the Faradaic efficiency increases, indicating that the photogenerated electrons are more effectively directed to the water reduction reaction compared to the competitive reduction of Zn^{2+}. An equilibrium situation is reached after 60 min, with the measurement of a stable photocurrent and an H_2 flow of approximately 2 μmol h^{-1} cm^{-2} during the next hour, and a Faradaic efficiency of 100% after 90 min.

These results can be easily explained by the energetic diagram shown in Figure 5b. In this diagram, the energy levels for both Zn^{2+} and H_2O reduction are included and we consider that both reduction reactions below [Eqs. (1) and (2)] are competitive.

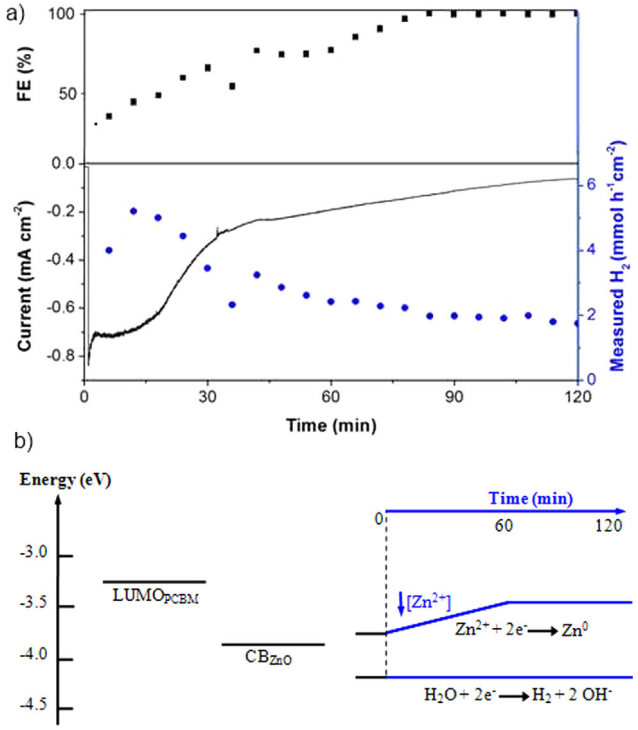

Figure 5. a) H_2 evolution for the system *x*-PEDOT/BHJ/AZO/C/Pt at pH 7, the measured photocurrent and the Faradaic efficiency. b) Energetic model of the photogenerated electrons at the electrode/electrolyte interface and the evolution of the energetic levels of the electrolyte with time, during H_2 generation. The redox potential of water reduction is corrected to pH 7.

$$2\,H_2O + 2e^- \rightarrow H_2 + 2\,OH^- \quad (1)$$

$$Zn^{2+} + 2\,e^- \rightarrow Zn^0 \quad (2)$$

The photogenerated electrons within the organic blend are collected at the LUMO band of the acceptor (PCBM). In contact with the organic blend (p-type semiconductor), the layer of AZO (n-type semiconductor) provides an excellent electron-selective contact for the formation of a rectifying p–n junction, which assists the extraction of the photogenerated electrons, with adequate energy to reduce both water to H_2 [Eq. (1)] and the Zn^{2+} cations of the AZO layer to Zn^0 [Eq. (2)]. Initially, the reduction of Zn^{2+} is favored (time 0 in Figure 5b), and the decrease of the Zn^{2+} concentration shifts the redox potential of Eq. (2) to higher values according to the Nernst equation (slope = 0.029 log[Zn^{2+}]) until equilibrium is reached and no further net Zn^{2+} reduction takes place. Then, all photogenerated electrons follow the desired hydrogen evolution reaction [Eq. (1)]. In the real device, the energetic diagram is more complex compared to that shown in Figure 5b, because the Zn^{2+} ions are present in the AZO layer (not in the electrolyte). In any case, the electrode surface is significantly affected as shown by surface analysis, and the simplified energy diagram of Figure 5b can reasonably explain the evolution of the electrode with time (Figure 5a). Although we use a C/Pt catalyst deposited by sputtering to analyze the response of the engineered photocathodes, to minimize losses at the semiconductor/solution interface, the basic device configuration is solution processed (photoactive material and selective contacts). Consequently, as far as the authors know, this is the first time that H_2 generation with a solution-processed organic photoelectrochemical system at neutral pH is reported.

Conclusions

We have developed an organic photoelectrochemical device able to reach photocurrents of more than 1 mA cm^{-2} at 0 V versus RHE, with reasonable stability under neutral pH conditions. The achieved performance is based on the use of an AZO nanoparticulated layer as an electron-selective contact, allowing device operation at neutral pH. Furthermore, we have clarified the origin of the evolution of photocurrent and Faradaic efficiency with time. The initial competitive reduction of both water and the AZO layer is responsible for the increased Faradaic efficiency from 60% to up to 100% after 90 min operation. Noteworthy after 1 h of operation of the device, a quite stable H_2 flow of approximately 2 μmol h^{-1} g^{-1} is obtained for 1 h. These results highlight the versatility and potential of organic photoelectrochemical devices as a real low-cost alternative for the generation of solar fuels.

Acknowledgements

We thank financial support from Generalitat Valenciana (ISIC/2012/008 Institute of Nanotechnologies for Clean Energies). We acknowledge the financial support of the European Community through the Future and Emerging Technologies (FET) programme under the FP7, collaborative Project contract n° 309223 (PHOCS). Additionally, the EU projects "Sunflower" (FP7-ICT-2011-7- contract num. 287594) and the SFUMATO—FUI Project AAP12 are acknowledged. A.G. would like to thank the Spanish Ministerio de Economía y Competitividad for a Ramón y Cajal Fellowship (RYC-2014-16809).

Keywords: hydrogen · organic photoelectrochemical cells · selective contacts · solar fuels · water splitting

[1] M. Meinshausen, N. Meinshausen, W. Hare, S. C. B. Raper, K. Frieler, R. Knutti, D. J. Frame, M. R. Allen, *Nature* **2009**, *458*, 1158 – 1162.
[2] S. Chu, A. Majumdar, *Nature* **2012**, *488*, 294 – 303.
[3] T. Hisatomi, J. Kubota, K. Domen, *Chem. Soc. Rev.* **2014**, *43*, 7520 – 7535.
[4] a) O. Khaselev, J. A. Turner, *Science* **1998**, *280*, 425 – 427; b) J. Luo, J.-H. Im, M. T. Mayer, M. Schreier, M. K. Nazeeruddin, N.-G. Park, S. D. Tilley, H. J. Fan, M. Graetzel, *Science* **2014**, *345*, 1593 – 1596.
[5] B. A. Pinaud, J. D. Benck, L. C. Seitz, A. J. Forman, Z. Chen, T. G. Deutsch, B. D. James, K. N. Baum, G. N. Baum, S. Ardo, H. Wang, E. Miller, T. F. Jaramillo, *Energy Environ. Sci.* **2013**, *6*, 1983 – 2002.
[6] F. C. Krebs, S. A. Gevorgyan, J. Alstrup, *J. Mater. Chem.* **2009**, *19*, 5442 – 5451.
[7] a) H. J. Park, J. Y. Lee, T. Lee, L. J. Guo, *Adv. Energy Mater.* **2013**, *3*, 1135 – 1142; b) Z. He, C. Zhong, S. Su, M. Xu, H. Wu, Y. Cao, *Nat. Photonics* **2012**, *6*, 591 – 595.
[8] S. Yanagida, A. Kabumoto, K. Mizumoto, C. Pac, K. Yoshino, *J. Chem. Soc. Chem. Commun.* **1985**, 474 – 475.
[9] a) O. A. El-Rashiedy, S. Holdcroft, *J. Phys. Chem.* **1996**, *100*, 5481 – 5484; b) E. Lanzarini, M. R. Antognazza, M. Biso, A. Ansaldo, L. Laudato, P. Bruno, P. Metrangolo, G. Resnati, D. Ricci, G. Lanzani, *J. Phys. Chem. C* **2012**, *116*, 10944 – 10949.
[10] A. Guerrero, M. Haro, S. Bellani, M. R. Antognazza, L. Meda, S. Gimenez, J. Bisquert, *Energy Environ. Sci.* **2014**, *7*, 3666.
[11] a) T. Bourgeteau, D. Tondelier, B. Geffroy, R. Brisse, R. Cornut, V. Artero, B. Jousselme, *ACS Appl. Mater. Interfaces* **2015**, *7*, 16395 – 16403; b) T. Bourgeteau, D. Tondelier, B. Geffroy, R. Brisse, C. Laberty-Robert, S. Campidelli, R. de Bettignies, V. Artero, S. Palacin, B. Jousselme in *Energy & Environmental Science, Vol. 6*, The Royal Society of Chemistry, London, **2013**, pp. 2706 – 2713; c) F. Fumagalli, S. Bellani, M. Schreier, S. Leonardi, H. Comas Rojas, A. Ghadirzadeh, G. Tullii, A. Savoini, G. Marra, L. Meda, M. Gratzel, G. Lanzani, M. T. Mayer, M. R. Antognazza, F. Di Fonzo, *J. Mater. Chem. A* **2016**, *4*, 2178 – 2187; d) M. Haro, C. Solis, G. Molina, L. Otero, J. Bisquert, S. Gimenez, A. Guerrero, *J. Phys. Chem. C* **2015**, *119*, 6488 – 6494; e) T. Bourgeteau, D. Tondelier, B. Geffroy, R. Brisse, S. Campidelli, R. Cornut, B. Jousselme, *J. Mater. Chem. A* **2016**, *4*, 4831 – 4839; f) H. Comas Rojas, S. Bellani, F. Fumagalli, G. Tullii, S. Leonardi, M. T. Mayer, M. Schreier, M. Gratzel, G. Lanzani, F. Di Fonzo, M. R. Antognazza, *Energy Environ. Sci.* DOI: 10.1039/c6ee01655c.
[12] P. Bornoz, M. S. Prevot, X. Yu, N. Guijarro, K. Sivula, *J. Am. Chem. Soc.* **2015**, *137*, 15338 – 15341.
[13] H. Kumagai, T. Minegishi, N. Sato, T. Yamada, J. Kubota, K. Domen, *J. Mater. Chem. A* **2015**, *3*, 8300 – 8307.
[14] M. Gaceur, S. B. Dkhil, D. Duche, F. Bencheikh, J.-J. Simon, L. Escoubas, M. Mansour, A. Guerrero, G. Garcia-Belmonte, X. Liu, M. Fahlman, W. Dachraoui, A. K. Diallo, C. Videlot-Ackermann, O. Margeat, J. Ackermann, *Adv. Funct. Mater.* **2016**, *26*, 243 – 253.
[15] T. K. A. Hoang, T. N. L. Doan, K. E. K. Sun, P. Chen, *RSC Adv.* **2015**, *5*, 41677 – 41691.
[16] B. Klahr, S. Gimenez, F. Fabregat-Santiago, J. Bisquert, T. W. Hamann, *Energy Environ. Sci.* **2012**, *5*, 7626 – 7636.
[17] R. Kou, Y. Shao, D. Wang, M. H. Engelhard, J. H. Kwak, J. Wang, V. V. Viswanathan, C. Wang, Y. Lin, Y. Wang, *Electrochem. Commun.* **2009**, *11*, 954 – 957.
[18] M. Haro, L. F. Velasco, C. O. Ania, *Catal. Sci. Technol.* **2012**, *2*, 2264 – 2272.
[19] a) G. Schön, *J. Electron Spectrosc. Relat. Phenom.* **1973**, *2*, 75 – 86; b) I. Valenti, S. Benedetti, A. di Bona, S. Valeri, *J. Phys. Chem. C* **2015**, *119*, 13743 – 13749.

Received: July 18, 2016
Published online on ■■ ■■, 0000

M. Haro, C. Solis, V. M. Blas-Ferrando, O. Margeat, S. B. Dhkil, C. Videlot-Ackermann, J. Ackermann, F. Di Fonzo, A. Guerrero, S. Gimenez**

■■ – ■■

Direct Hydrogen Evolution from Saline Water Reduction at Neutral pH using Organic Photocathodes

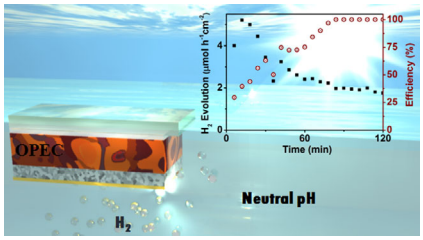

Neutral pH: The development of an organic photocathode with engineered interfacial selective layers is described towards direct H_2 generation from saline water at neutral pH using solar energy. The electron-selective layer based on ZnO doped with Al (AZO) is the key towards operation under neutral pH conditions. Once the system is at equilibrium, a flow of approximately 2 μmol h^{-1} is measured over 1 h at 0 V versus RHE.